ELSEVIER

Journal of Nuclear Materials 250 (1997) 164–170

journal of nuclear materials

# Generalized creep model of Zircaloy-4 cladding tubes

Young Suk Kim *

*Korea Atomic Energy Research Institute, PO Box 105, Yusong-gu, Taejon 305-600, South Korea*

Received 27 November 1996; accepted 3 August 1997

**Abstract**

Zircaloy-4 cladding tubes with different area reductions at the final cold working were subjected to creep testing at temperatures of 350 to 500°C. The creep testing was carried out mainly at the biaxial stress state. The creep rate and creep strain of the Zircaloy-4 cladding tube increased with increasing area reduction at the final cold working. The creep model was derived to cover the effect of area reduction and then verified by using supplementary creep data obtained at 350°C and 138 MPa. Furthermore, this generalized creep model was verified to well describe the thermal creep of Duplex tubes and low Sn Zircaloy-4 tubes. The creep rate of Zircaloy-4 cladding tubes followed the exponential stress dependence, not the power law creep. The creep activation energy was determined to be 60 kcal/mol, leading to the conclusion that creep is controlled by dislocation creep. Thus, it is suggested that the increase of creep rates and creep strains with the increase in cold working is due to an enhanced climb rate arising from the increased concentration of vacancy. © 1997 Elsevier Science B.V.

## 1. Introduction

Creep of Zircaloy-4 cladding is one of the important properties determining the gap distance between fuel and cladding, and influencing the heat transfer from fuel to coolant. Therefore, an understanding of the creep behavior of Zircaloy-4 cladding is required to predict safely and reliably the thermal performance and mechanical integrity of fuel rods. Researches on the creep of Zircaloy-4 have been conducted [1,2] but it is not clear what the main process controlling the creep rate of Zircaloy-4 is. Kalstrom showed that the creep of Zircaloy-4 is anisotropic and varies with the area reduction in the final rolling though the texture effect is trivial compared to the area reduction effect [1]. However, Murty insisted that the creep rate of Zircaloy-4 is determined by the texture and, when applicable, grain shape anisotropy [2].

Since the creep of Zircaloy-4 is related to the movement of dislocation, however, attention should instead be paid to the area reduction at the final cold working. This is due to the fact that the mobility of dislocation is strongly affected by the area reduction that Zircaloy-4 tube undergoes during manufacturing. The purpose of this study is to systematically investigate the effect of the area reduction on the creep of Zircaloy-4 cladding tubes and to derive a generalized creep model that can be applied to all Zircaloy-4 cladding tubes. The Zircaloy-4 tubes used in this study were subjected to different area reductions at the final pilger pass as shown in Table 1. On the other hand, at the final annealing, tube A was subjected to a stress relieving treatment while the others underwent a partially recrystallized treatment with an identical degree of recrystallization among them. Thus, tube A had greater strength than the others which showed almost the same yield of strength among them. To verify a derived creep model, complementary creep testing was additionally conducted on tube B at 350°C and 138 MPa. Furthermore, the creep behavior of Duplex tubes and low Sn Zircaloy-4 were investigated to prove the generality of the derived creep model.

* Tel.: +82-42 868 2359; fax: +82-42 868 8346; e-mail: yskim1@nanum.kaeri.re.kr.


*PII* S0022-3115(97)00261-4

## 2. Experimental procedures

### 2.1. Cladding tubes used

Four different Zircaloy-4 cladding tubes were used in this study, referred to as tubes A, B, C and D, as shown in Table 1. To identify the effect of the area reduction, these tubes were subjected to various area reductions from 64.3 to 81.7% at the final pilger pass. It is worth noting that all tubes except tube A underwent a partially recrystallized treatment, leading to identical yield strength and texture among them. Furthermore, the measurement of the degree of recrystallization by TEM showed that their degree of recrystallization was identical as shown in Table 1. TEM foils with an area of 20 000 to 30 000 $\mu m^2$ were shown to obtain a highly representative value for the degree of recrystallization. However, tube A with the largest area reduction had a stress relieving treatment at the final annealing, resulting in a yield strength 20–25% higher than other tubes with partially recrystallized treatment.

Duplex tubes whose OD surfaces were covered with corrosion resistant zirconium alloys were used to investigate the applicability of a derived creep model along with low Sn Zircaloy-4: D1 (Zr–2.5% Nb), D2 (Zr–0.4% Fe–0.5% Sn), and D3 (Zircaloy-4 + 1% Nb). The details of their chemical compositions are reported elsewhere [3].

### 2.2. Creep testing

Biaxial creep testing was conducted at 350 and 400°C by internal pressurization of 20 cm long tubes where the hoop stress changed from 80 to 150 $N/mm^2$. The temperature along a tube was controlled within $\pm 1$°C while the tube pressure was monitored by a transducer for the duration of the exposure. The creep strain was measured by measuring the change of the tube OD periodically. On the other hand, the creep testing at 500°C was conducted with the ratio of tangential stress and axial stress changing from 0 to 2 by using a lever arm machine (the ATS model 2330 with the lever arm ratio of 20 to 1).

## 3. Results and discussion

### 3.1. Creep of Zircaloy-4 cladding

Figs. 1 and 2 show the creep stains of Zircaloy-4 cladding tubes over time at 400 and 350°C, respectively. The creep strain and rate of Zircaloy-4 cladding increased with increasing area reduction at the final cold working: tube A with 81.7% area reduction showed the largest creep strain and creep rate, while tube D with 60.3% area reduction had the lowest creep strain and creep rate. The same trend was also confirmed by the creep testing at the hoop stresses of 100 and 120 $N/mm^2$ and 400°C. It is worth noting that tubes A and B with a similar area reduction showed similar creep strains and the very same creep rate, despite the difference in the final annealing treatment and the former cold working processes. Furthermore, the larger creep strains and creep rate of tube B, as opposed to tube C, lead to the definitive conclusion that the area reduction is a main controlling factor in determining the creep behavior of Zircaloy-4. This is due to the fact that the only manufacturing variable between tubes B and C is the area reduction at the final cold working.

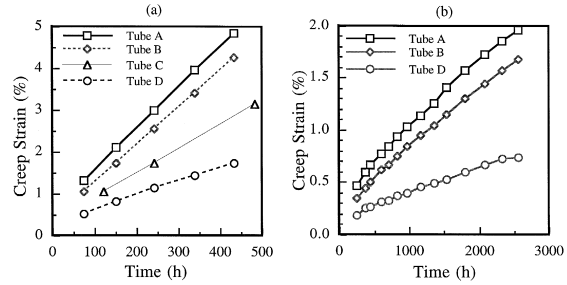


Fig. 1. Creep strain of four different of Zircaloy-4 tubes at 400°C and at (a) 150 MPa and (b) 80 MPa.

Table 1
Characteristics of Zircaloy-4 cladding tubes

| Item | Tube A | Tube B | Tube C | Tube D |
|---|---|---|---|---|
| (1) Dimension (OD × W) | 9.5 × 0.58 | 9.5 × 0.64 | 10.75 × 0.73 | 9.5 × 0.64 |
| (2) Area reduction at final cold working (%) | 81.7 | 80.3 | 74.7 | 64.3 |
| (3) Final heat treatment | SR[a] | PR[b] | PR | PR |
| (4) Degree of recrystallization | – | 13–24 | 13–24 | 10–24 |
| (5) Kearns No. ($f_r$) | – | 0.52 | 0.56 | 0.52 |
| (6) Yield strength at RT ($N/mm^2$) | 652 | 507 | 493–517 | > 471 |
| (7) Tensile strength at RT ($N/mm^2$) | 849 | 709 | 681–705 | > 664 |

[a] Stress relieved.
[b] Partially recrystallized.

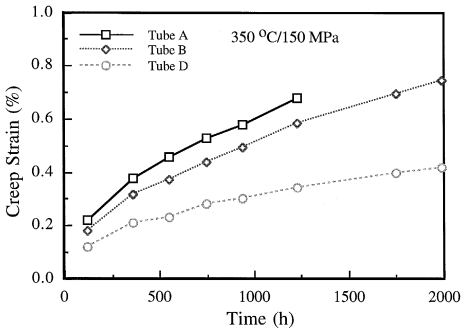


Fig. 2. Creep strain of four different Zircaloy-4 tubes at 350°C and 150 MPa.

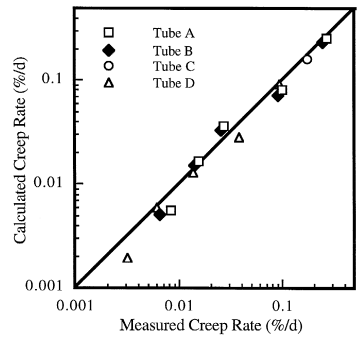


Fig. 4. Comparison of the measured and calculated creep rates for four different Zircaloy-4 tubes.

Tubes B and D had a similar texture but showed quite different creep strains and rates. This fact suggests that the effect of texture on the creep behavior of Zircaloy-4 is insignificant compared to the area reduction effect. Therefore, the texture effect was disregarded in developing a creep model.

### *3.2. Modeling of Zircaloy-4 creep*

An empirical creep equation was derived using a Dorn's model [4], in which the creep rate and strain at the mid-wall of a Zircaloy-4 tube were expressed as a function of effective stress. The mid-wall strain was calculated from the OD creep strain by assuming a constant volume under plastic deformation [5]. The creep equation to best fit the creep behavior of tube B was expressed as

$$\varepsilon_t = \varepsilon_p^0\left(1 - \exp\left(-34.13\dot{\varepsilon}\sqrt{t}\right)\right) + \dot{\varepsilon}t, \qquad (1)$$

$$\dot{\varepsilon}_t = c_1 \exp(-30\,084/T\ (\mathrm{K}))\exp(3300\sigma_{\mathrm{eff}}/E), \qquad (2)$$

where $\varepsilon_t$ is the total creep strain (%), $\dot{\varepsilon}$ is the steady state creep rate (%/d), the primary creep constant $\varepsilon_p^0 = 4.84 \times 10^{-3}\sigma_{\mathrm{eff}}$ (%), the constant $c_1 = 1.72 \times 10^{16}$ (%/d), the effective stress $\sigma_{\mathrm{eff}} = 1/\sqrt{2}\,[(\sigma_t - \sigma_r)^2 + (\sigma_r - \sigma_{ax})^2 + (\sigma_{ax} - \sigma_t)^2]^{1/2}$ (N/mm$^2$) and $E$ is an elastic modulus of Zircaloy-4 (N/mm$^2$). It should be noted that the primary creep constant, $\varepsilon_p^0$, increases with $\sigma_{\mathrm{eff}}$. The creep rates and strains calculated by Eqs. (1) and (2) agreed well with the measured ones taken from tube B, as shown in Fig. 3.

With an aim to develop a generalized creep model that can describe the creep behavior of not only tube B but all four Zircaloy-4 tubes, Eqs. (1) and (2) were adjusted to introduce a variable of the area reduction. This is because the creep rate and strain of Zircaloy-4 cladding tube increase proportionally with an increase in the area reduction at the final cold working, as shown in Figs. 1 and 2. The generalized creep equations were represented as follows:

$$\dot{\varepsilon}_g = \mathrm{RA}^2/(1 - \mathrm{RA}^2)9.477 \times 10^{15} \times \exp(-30\,084/T\ (\mathrm{K}))\exp(3300\sigma_{\mathrm{eff}}/E), \qquad (3)$$

$$\varepsilon_{g,t} = 6.027 \times 10^{-3}\mathrm{RA}\,\sigma_{\mathrm{eff}} \times \left(1 - \exp\left(-34.13\dot{\varepsilon}\sqrt{t}\right)\right) + \dot{\varepsilon}t, \qquad (4)$$

where $\varepsilon_{g,t}$, $\dot{\varepsilon}_g$ and RA represent the generalized total creep strain, the generalized creep rate and the area reduction at the final cold working (%), respectively. The main feature of this generalized creep model is that the primary creep strain and steady state creep rate vary as a function of the area reduction, RA, as shown in Eqs. (3) and (4). A comparison of the measured creep rates and the predicted

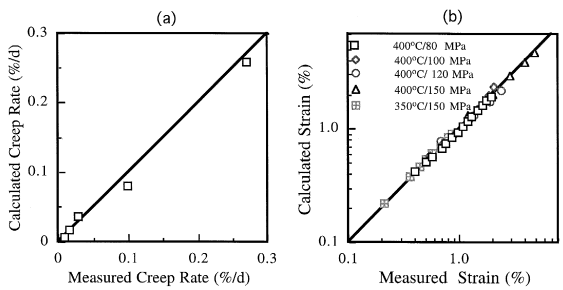


Fig. 3. Comparison of the calculated creep rates (a) and strains (b) with the measured ones of tube B.

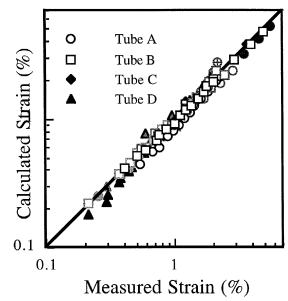


Fig. 5. Comparison of the measured and calculated strains for all four Zircaloy-4 tubes.

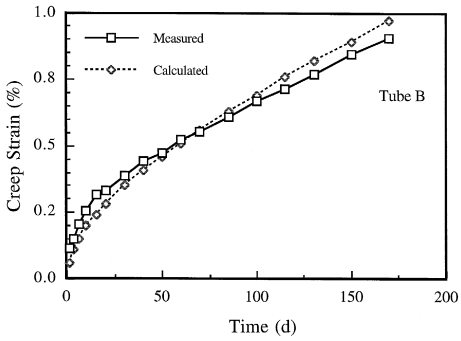


Fig. 6. The verification of the generalized creep model by comparing the calculated and the measured strains taken at 138 MPa and 350°C for tube B.

ones was made for all four Zircaloy-4 cladding tubes, as shown in Fig. 4. The predicted creep rates obtained by this generalized creep rate agreed excellently with the measured ones. Furthermore, the total creep strains determined using Eq. (4) agreed well with the measured ones taken from all four kinds of Zircaloy-4 cladding tubes in all creep testing conditions, as shown in Fig. 5. Consequently, it is concluded that the generalized creep model can predict well the creep behavior of any Zircaloy-4 cladding tube if its area reduction at the final cold working is known.

### *3.3. Verification of the generalized creep model*

Complementary biaxial creep testing was carried out additionally for tube B at 350°C and 138 MPa hoop stress to verify the generalized creep model. Fig. 6 shows a comparison of the measured and calculated creep strains. Even at a hoop stress of 138 MPa and 350°C, this generalized creep model was verified to predict well the creep behavior of Zircaloy-4.

To see if the generalized creep model is applicable to Duplex tubes and low Sn Zircaloy-4 tubes, biaxial creep testing was conducted on them as well as tube B, at 350 and 400°C. The tangential stress was kept constant at 138 or 150 MPa. Duplex tubes and low Sn Zircaloy-4 tube showed enhanced creep strains and rates compared to tube B as shown in Fig. 7. Among the Duplex tubes, D1 showed the highest creep strain and rate while D2 had the lowest creep rate and strain. According to the generalized creep equations (Eqs. (3) and (4)), Duplex tubes and low Sn Zircaloy-4 must have undergone a greater area reduction at the final cold working compared to tube B. The area reductions of these Duplex tubes and low Sn Zircaloy-4 were calculated based on the measured creep rates and their relative ratios over the creep rates of tube B that was taken at 350°C and 138 MPa (see Table 2). However, since the detailed manufacturing procedure of Duplex tubes and low Sn Zircaloy-4 is not known to us, it remains to be confirmed how correct the calculated area reduction for Duplex tubes and low Sn Zircaloy-4 is.

Table 2
Measured creep rates and calculated area reduction of Duplex tubes and low Sn Zircaloy-4

| Tubes | Creep rate at mid-wall(%/d) | Creep rate ratio | Calculated area reduction (%) |
|---|---|---|---|
| D1 | $8.92\times10^{-3}$ | 2.5 | 91.2 |
| D3 | $6.59\times10^{-3}$ | 1.8 | 88.5 |
| D3 | $5.35\times10^{-3}$ | 1.5 | 86.5 |
| Low Sn Zry-4 | $4.33\times10^{-3}$ | 1.2 | 84.6 |
| Tube B | $3.57\times10^{-3}$ | 1 | 80.3[a] |

[a] Measured value.

By using these calculated area reductions, their creep rates were calculated and compared with the measured ones at 400°C. The calculated creep rates of Duplex tubes and low Sn Zircaloy-4 agreed well with the measured ones at 400°C and 150 MPa, as shown in Fig. 8. In addition, when the measured creep strains of Duplex tubes and low Sn Zircaloy-4 were compared with the calculated ones, as shown in Fig. 9, the calculated creep strains agreed with the measured ones, also. Conclusively, the results shown in Figs. 7–9 prove that the generalized creep model is

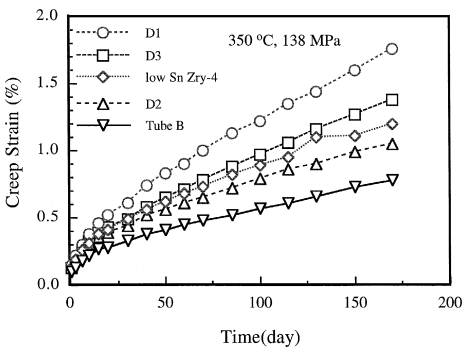


Fig. 7. Creep strain of Duplex tubes, D1, D2 and D3, and low Sn Zircaloy-4 at 350°C and at hoop stress of 138 MPa.

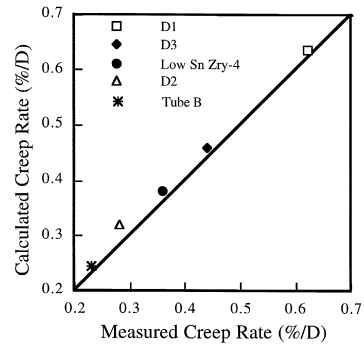


Fig. 8. Comparison of the calculated creep rates with the measured ones of Duplex tubes, low Sn Zircaloy-4 and tube B at 400°C and 150 MPa.

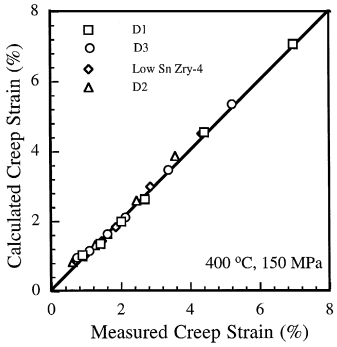


Fig. 9. Comparison of the calculated and measured creep strains for Duplex tubes, D1, D2 and D3, and low Sn Zircaloy-4 tube at 400°C and 150 MPa.

applicable to both the Duplex tubes and low Sn Zircaloy-4 as well.

The main feature of this generalized creep model is the fact that the creep rate increases exponentially with equivalent stress. In other words, it does not follow a power law creep as reported by Murty where the creep rate increases with the stress of the exponent $n$ [3]. To confirm that the creep rate of Zircaloy-4 follows the stress dependence, additional supplementary creep testing was conducted on tubes B and D at 500°C, with the ratio of tangential stress and axial stress changing from 0 to 2. When the log–log plot of the creep rate versus stress was made, the slope, $n$ was not constant but changed with the applied stress conditions, as shown in Fig. 10. However, when a semi-log plot of the creep rate versus equivalent stress was made, a linear relationship was observed, regardless of the stress state, while the value of $n$ was determined to be 0.045 as shown in Fig. 11. By incorporating 0.045 for $n$ and the calculated value of elastic modulus at 500°C into Eq. (3), an exponential constant of 3000 was obtained in comparison to the 3300 as determined in the generalized equation (Eq. (3)). It is not clear if the difference in the exponential constant may be related to a partial recrystallization during creep testing or to the uncertainty of the calculated elastic modulus and experimental error. A conclusion can nevertheless be drawn, however, that the creep rate of Zircaloy-4 follows an exponential function of equivalent stress and not a power law creep.

### *3.4. Creep controlling mechanism of Zircaloy-4*

The activation energy for the creep of Zircaloy-4 cladding tubes turned out to be 60 kcal/mol as shown in Eq. (3). This is in quite good agreement with the creep activation energy reported by Murty [4] and Lyashenko [6]. Furthermore, as this value is very consistent with the self-activation energy of zirconium in α-zirconium, 69

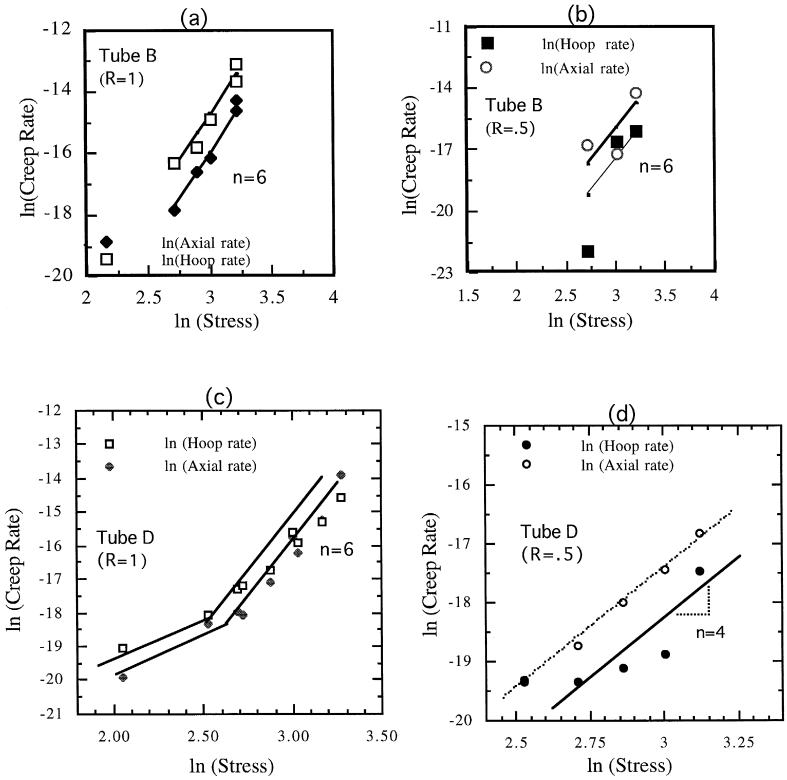


Fig. 10. Log–log plot of the hoop and axial creep rates for tubes B and D under an $R\ (=\sigma_\theta/\sigma_z)$ of 1 and 0.5.

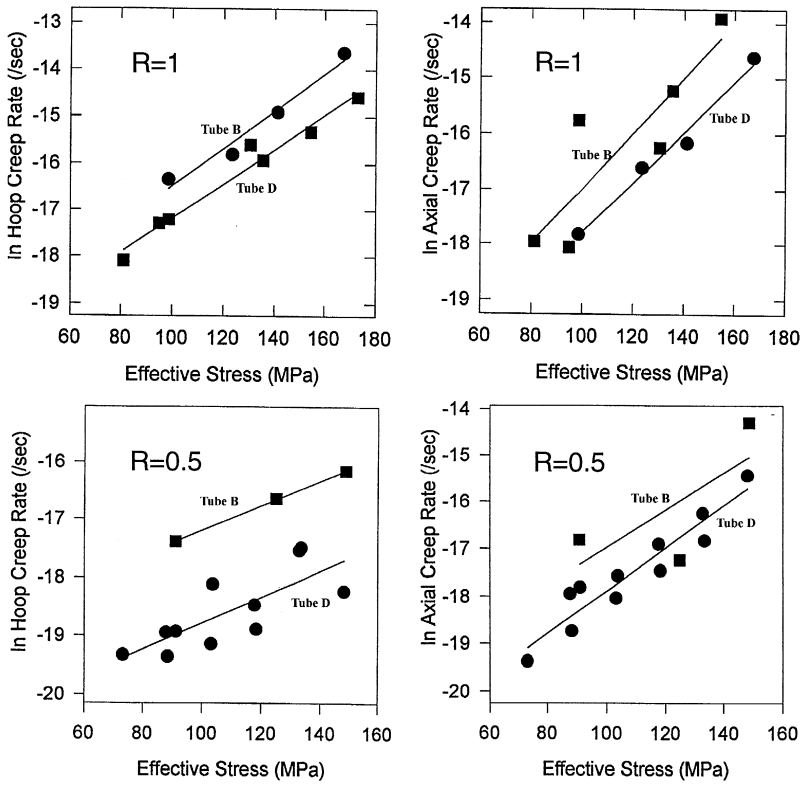


Fig. 11. Semi-log plot of the creep rate versus effective stress for tubes B and D under an $R\ (=\sigma_\theta/\sigma_z)$ of 1 and 0.5.

kcal/mol [7], the creep rate of Zircaloy-4 conclusively is controlled by zirconium diffusion. In other words, it is concluded that the rate of dislocation climb that is affected by zirconium diffusion determines the creep rate of Zircaloy-4. Holmes already suggested this assumption based simply on the calculated activation energy [8] but failed to show any evidence to support his hypothesis.

The larger the amount of cold working at the final pass, the higher the concentration of vacancy becomes [9]. Therefore, the creep rate of Zircaloy-4, is expected to increase with increasing vacancy concentration. Therefore, the proportional increase of the creep rate of Zircaloy-4 cladding with the area reduction at the final cold working stage provides evidence that the creep of Zircaloy-4 is controlled by dislocation climb. It should be noted that tubes B, C and D were subjected to different area reductions at the final cold working, followed by partial recrystallized treatment with an identical degree of recrystallization among them. Therefore, the faster creep rate of tube B must prove that the creep rate of Zircaloy-4 cladding is determined mainly by the area reduction at the final cold working, leading to an increasing rate of dislocation climb.

## 4. Conclusion

This study demonstrated that the creep stain and rate of Zircaloy-4 increased proportionally with the increasing area reduction at the final pilger pass. A generalized creep model was derived to describe the creep behavior of four different kinds of Zircaloy-4 cladding by introducing the area reduction effect shown in Eqs. (3) and (4).

By using complementary creep data taken at 350°C and 138 MPa, this generalized creep model was verified to predict well the creep behavior of Zircaloy-4 cladding tubes. Furthermore, this model was confirmed to explain well the creep behavior of all Duplex tubes and low Sn Zircaloy-4 tubes. The creep rate of Zircaloy-4 cladding tubes followed the exponential equivalent stress dependence, not a power law stress dependence creep. The creep activation energy was 60 kcal/mol, leading to the conclusion that creep is controlled by dislocation climb. Thus, increasing creep rates and creep strains with the increasing area reduction at the final cold working are due to the enhanced climb rate arising from the increased concentration of vacancy at higher cold working.

## References

[1] K. Kallstrom, T. Andersson, A. Hofvenstam, in: Zirconium in Nuclear Application, ASTM-STP 551, eds. J.H. Schemel and H.S. Rosenbaum (American Society for Testing and Materials, Philadelphia, PA, 1974) p. 160.

[2] K.L. Murty, B.V. Tanikella, J.C. Earthman, Acta Metall. Mater. 42 (1994) 3653.

[3] O.A. Besch, S.K. Yagnik, K.N. Wood, C.M. Eucken, E.R. Bradley, Abstracts of 11th Int. Symp. on Zirconium in the Nuclear Industry, 1995, p. 38.
[4] K.L. Murty, G.S. Clevinger, T.P. Papazogloa, Trans. of the 4th Int. Conf. on Structural Mechanics in Reactor Technology, Vol. C, SF, CA, 1977, p. C3/4.
[5] Y.S. Kim, Korea Atomic Energy Research Institute Report, KAERI/RR-933/90.
[6] V.S. Lyashenko, V.N. Bykor, L.V. Pavlinov, Phys. Metal Metallogr. 8 (1960) 40.
[7] G.M. Hood, memo to Y.S. Kim, RMR-95-378, 1995.
[8] J.J. Holmes, J. Nucl. Mater. 13 (1964) 137.
[9] R.W. Cahn, Physical Metallurgy (Elsevier, New York, 1970) p. 857.